

Cyclosporin A promotes invasion and migration of extravillous trophoblast cells derived from human induced pluripotent stem cells and human embryonic stem cells

Jiaxing Wang

The First Affiliated Hospital of Hainan Medical University

Ping Long

The First Affiliated Hospital of Hainan Medical University

Shengnan Tian

The Second Hospital of Shandong University

Weihua Zu

The First Affiliated Hospital of Hainan Medical University

Jing Liu

The First Affiliated Hospital of Zhengzhou University

Bangyong Wu

The Affiliated Hospital of Hainan Medical University

Jilong Mao

The First Affiliated Hospital of Hainan Medical University

Dan Li

Haikou Women & Children Hospital

Yanlin Ma

The First Affiliated Hospital of Hainan Medical University

Yuanhua Huang (✉ 13036095796@163.com)

The first Affiliated Hospital of Hainan Medical University

Research

Keywords: Extravillous trophoblast, cyclosporin A, human induced pluripotent stem cells, human embryonic stem cells

Posted Date: May 11th, 2020

DOI: <https://doi.org/10.21203/rs.3.rs-25667/v1>

License: © ⓘ This work is licensed under a Creative Commons Attribution 4.0 International License.

[Read Full License](#)

Abstract

Background

Extravillous trophoblast (EVT) cells play an essential role in the maternal-fetal interaction. Although abnormal development and function of EVT cells, including impaired migration and invasion capability, are believed to be etiologically linked to severe pregnancy disorders including pre-eclampsia (PE), the associated molecular mechanisms are not clear ascribed to the lack of an appropriate cell model in vitro. Cyclosporine A (CsA) is a macrolide immunosuppressant and is also used in clinic to improve pregnancy outcomes. However, whether CsA has any effects on the function of EVT cells has not been well investigated.

Methods

In this study, we induced differentiation of human induced pluripotent stem cells (hiPSCs) and human embryonic stem cells (hESCs) into EVT cells (hiPSC-EVT and hESC-EVT cells, respectively) by Y27632, NRG1, A83-01 and matrigel, and collected these derived EVT cells by flow cytometry for sorting cells positive for double HLA-G and KRT7, which are EVT markers. We then investigated the effects of CsA on the invasion and migration of these derived EVT cells.

Results

We found that the hiPSC-EVT and hESC-EVT cells expressed high levels of the EVT markers such as KRT7, ITGA5 and HLA-G but low levels of OCT4, a stem cell marker, and that CsA significantly promoted the invasion and migration of hiPSC-EVT and hESC-EVT cells.

Conclusions

We successfully generated hiPSC/hESC-derived human EVT cells, which may be applicable for investigating the remodeling process of spiral arteries remodeling and the possible mechanisms of EVT-related diseases in vitro. Furthermore, our findings provide direct evidence that CsA regulates the function of EVT cells and molecular basis by which CsA may be used to treat pregnancy complications in clinic associated with deficient EVT function.

Introduction

Human placenta formation is a complex and sophisticated process that is initiated by trophoblasts. After fertilization, the trophoblast (TE) cells give rise to trophoblasts, including cytotrophoblast (CTB), syncytiotrophoblast (STB) and extravillous trophoblast (EVT) [1]. In the distal end of the anchoring villus, the proliferative cell columns differentiate into EVTs. Following that, the EVT cells invade the uterine

decidua, the muscular layer (inside 1/3) and the spiral arteries [2], which plays an important role in gradual displacement of vascular endothelial cells and in the endovascular remodeling of the spiral artery. The EVT-associated process transforms spiral arteries from high resistance and low flow to low resistance and high flow blood vessels, and establishes maternal fetal blood circulation to ensure adequate supply of oxygen and nutrients to fetus during pregnancy [3–5]. Previous studies have shown that abnormal changes in EVT invasion lead to pregnancy-related diseases such as pre-eclampsia (PE), fetal growth restriction (FGR) and early recurrent spontaneous abortion (RSA) [6–8], while the exact mechanisms by which EVT functional deficiency causes these diseases are not clear, in part due to the lack of a valid in vitro model to study the physiology and pathophysiology of EVT cells.

Currently, the study of trophoblast differentiation and placental formation mainly focuses on animal models, primary human trophoblast cells, choriocarcinoma cell lines and BMP4-induced differentiation [9]. However, these models do not completely recapitulate the mechanisms of human trophoblast differentiation or placenta formation due to their respective limitations. For instance, although the mouse model mimics the development of trophoblast and placental development in vitro, there are significant species differences in the extent of EVT cells invasion into the uterus [10–11]. Also, the primary trophoblast cells isolated from the first-trimester placenta rapidly differentiate and do not survive for a long period of time in vitro [12–13]. In addition, the ethical issues have limited the use of primary cultured trophoblast cells isolated from human placenta. Based on the above limitations, pluripotent stem cells (hiPSCs) or human embryonic stem cells (hESCs) treated with BMP4 for differentiation have been introduced. This model has several significant advantages: first, hiPSCs and hESCs can be cultured for a long time and remain in the undifferentiated state [14]; second, hiPSCs and hESCs have the ability to differentiate into trophoblasts [15]. However, the trophoblast cells derived from hiPSCs and hESCs remain controversial with their heterogeneity. In 2018 Okae et al generated human trophoblast stem (TS) cells from the first-trimester placentas and blastocysts, and showed that TS cell has the ability to differentiate into EVT and syncytiotrophoblast (ST) [16]. This study also showed that these trophoblasts have expression pattern similar to the primary cultured EVT cells [16]. However, the generation of this model still exhibits ethical limitations. Similarly, the establishment of the artificial mini-placenta model may provide a good system for trophoblast development [17]. Nevertheless, it is still unclear whether the artificial mini-placenta model is currently available and can mimic the differentiation and the regulatory mechanisms of the first trimester trophoblasts in vitro.

Cyclosporin A (CsA) is a macrolide immunosuppressant and mainly used for immunological rejection after organ transplantation and treatment of autoimmune diseases. Previous studies have shown that CsA enhances Th2-type cytokine production at the maternal-fetal interface in human first trimester [18], thus it might provide benefits for patients with pregnancy related diseases such as spontaneous pregnancy wastage. Previous surveys have also suggested that low doses of CsA motivate the proliferation, invasion and migration of human first-trimester trophoblasts via activating the mitogen-activated protein kinase (MAPK) signaling pathways [19–21]. Consistent with the above observations, animal experiments also suggested that low concentration of CsA improve pregnancy outcomes by promoting the proliferation and invasiveness of murine trophoblasts and inducing maternal tolerance to

the allogeneic fetus in abortion-prone matings [22]. However, the effects of CsA on EVT function and its regulation mechanism have not been defined during early human pregnancy.

In the present study, we induced differentiation of hiPSC and hESC into EVT (hiPSC-EVT and hESC-EVT, respectively) cells with several factors, and characterized these derived EVTs. We further examined the effects of CsA on the invasion and migration of these hiPSC-EVT and hESC-EVT cells.

Materials And Methods

Ethic statement

The study proposal was approved by the Ethics Committee of The First Affiliated Hospital of Hainan Medical University (2017-KY-001). All donors signed informed consent forms in this research.

Isolation and culture of human primary trophoblast cells

The primary trophoblasts were isolated and cultured from human placentas of healthy women as previously described [23–24]. Briefly, placental tissues between 6 ~ 9 weeks of gestation were cut into a size of 1 mm³, and digested three times in a solution with 0.25% Trypsin and Accutase (1:1) at 37 °C for 10 min. Then, the digestion liquid was collected in a 50 ml tube with an equal volume of Horse serum, filtered through a 100 µm strainer and centrifuged at 4 °C (1200 × g, 15 min). Cell suspension was then added to the Percoll density gradient (30%-50%) for centrifugation at 4 °C (1200 × g, 20 min). The layer containing trophoblast cells was collected between the 30% and 50% Percoll density (1.048–1.062 g/ml), suspended in DMEM-F12 medium containing 10% FBS and centrifuged at 4 °C (1200 × g, 5 min). The resulting trophoblast cells were transferred into DMEM-F12 medium containing with 10% FBS and 1% penicillin-streptomycin (10000 units/ml -10000 µg/ml each). Finally, trophoblast cells were transferred to six-well plates coated with matrigel (200 µl in 36 ml DMEM-F12) at density of 5 × 10⁵ cells/ml, and cultivated at 37 °C in 5% CO₂. After 5–12 h culture, the non-adherent cells were removed.

Culture of hESCs, hiPSCs and HTR-8/SVneo cells

HESCs and hiPSCs were cultured according to the protocols developed by Hainan Provincial Key Laboratory for Human Reproductive Medicine and Genetic Research [25]. Briefly, hiPSCs (from the first-trimester human placenta villus) and hESCs (H1 line obtained from Pei's labs with WiCell approval) were cultured under mTeSR1, and passaged with EDTA every 2–3 days. HTR-8/SVneo cells (a gift from Xiao's labs with WiCell approval) were incubated in RPM1640 medium containing 10% FBS. HTR-8 cells were passaged every 2–3 days. Cells after 2–3 passages were used in this study.

Differentiation of hESCs and hiPSCs into EVT cells

Differentiation of hESCs and hiPSCs into EVT cells was induced as previously reported [16]. Briefly, hESCs and hiPSCs were reached to 75%~80% confluence in the mTeSR1 medium, and digested with EDTA-TrypLE for 3 min in a CO₂ incubator (5% CO₂; 37 °C). To induce EVT differentiation, hESCs and

hiPSCs were seeded at a density of $1.5 \sim 2.0 \times 10^5$ cells per well in a 6-well plate pre-coated with 1 ml matrigel. Cells were incubated in 2 mL EVT basal medium (DMEM-F12 containing 0.1 mM 2-mercaptoethanol, 0.5% Penicillin-Streptomycin, 0.3% BSA, and 1% ITS-X supplement) supplemented with 100 ng/ml human neuregulin-1 (NRG1), 7.5 mM A83-01, 2.5 mM Y27632, and 4% Knock Out Serum Replacement (KSR). Then matrigel was added in this medium as a final concentration of 2%. At day 3, the medium was substituted for the above medium without NRG1, and matrigel was added as a final concentration of 0.5%. At day 6, the medium was substituted for the medium without NRG1 and KSR, and matrigel was added as a final concentration of 0.5%. Cells were analyzed by flow cytometry at day 9.

Flow cytometry

EVT cells derived from hESCs and hiPSCs, respectively, named hESC-EVT and hiPSC-EVT cells, were digested at 37 °C for 5–10 min in a solution containing Trypsin and Accutase (1:1). The resulting cells passed through a 70 mm mesh filter, and suspended in PBS. Then cells were incubated with a PE-conjugated anti-HLA-G antibody (1:50) and an APC-conjugated anti-KRT7 antibody (1:50) at 37 °C for 30 min for flow cytometric analysis and sorting. Cells without incubation with these antibodies were used as a negative control. The HLA-G positive and KRT7 positive cells (double positive cells) were sorted through flow cytometry FACS Aria II (BD Biosciences), and data were analyzed by FlowJo_V10 software (BD Biosciences). All reagents used are summarized in Table S1.

Immunofluorescence staining

The double positive cells were fixed in a solution of methanol and acetone (1:1) at -20 °C for 30 min. After wash with PBS, cells were incubated for 1 h at room temperature with the blocking buffer (5% BSA and 0.1% Tween-20 in PBS), then incubated overnight at 4 °C in the following primary antibodies: anti-KRT7 (1:200), anti-HLA-G (1:200), anti-OCT4 (1:200), anti-ITGA5 (1:200). After then, cells were incubated for 1 h at room temperature with appropriate Alexa Fluor 568-conjugated or Fluor 488-conjugated secondary antibodies. Nuclei were stained with DAPI. Immunofluorescence staining images were obtained with a Laser Scanning Confocal Microscope (FV1000, Olympus, Japan). All antibodies used are summarized in Table S2.

Reverse transcription and quantitative polymerase chain reaction (RT-qPCR)

According to the Trizol Reagent manufacturer's protocol, total RNA was isolated from cells. The purity and concentration of total RNA were tested with a NanoDrop 2000 Spectrophotometer (Thermo Fisher Scientific). The cDNA was synthesized from total RNA using PrimeScript II. With the SYBR Premix Ex TaqII, real-time PCR reaction was performed. The expression level of target genes was determined by the $\Delta\Delta C_t$ method, with glyceraldehyde 3-phosphate dehydrogenase (GAPDH) as the internal control. The sequences of primers used are summarized in Table S3.

Invasion assay

Cell invasion was evaluated by transwell chamber assay as previously described [19]. Briefly, the upper inserts (8 μm pore size, 6.5 mm diameter, Corning, USA) pre-coated with 200 μl matrigel were placed at 37 °C for 1 h in a CO₂ incubator. Both hESC-EVT and hiPSC-EVT (2.5×10^4 cells/well) cells were treated with various concentrations of CsA (0, 1.0, and 10 μM , respectively) in the upper chamber after the matrigel were removed. The lower chamber was added with 600 μL EVT basal medium supplemented with 10% FBS. Cells were cultured in 5% CO₂ and 37 °C for 48 h. The cells without invading the filters were removed with a cotton swab from the upper surfaces. The inserts were fixed for 30 min with 4% paraformaldehyde, and then stained with Giemsa Stain solution at room temperature for 10 min. Staining was captured with Olympus microscope (BX51 + DP72, Olympus, Japan). The cells invaded the filters to the lower surfaces were counted in 6 randomly selected at a magnification of $\times 400$, and non-overlapping fields. Each experiment was performed in triplicate, and duplicated at least 3 times. The migration index was determined by the rate of the percentage of cell invasion from the varied concentrations of CsA to that of the vehicle.

Scratch wound healing assay

Cell migration was performed by the scratch wound healing assay as described previously [19]. Briefly, hESC-EVT and hiPSC-EVT cells were grown to 75%~80% confluency and dissociated with Trypsin and Accutase for 5–10 min at 37 °C. Then, cells were seeded in a culture-insert (Ibidi, Germany) at a concentration of 5×10^5 cells/well, and cultured for 12 h at 37 °C until cells reached confluency. The wound formed after removal of the insert. After then, cells were transferred into EVT medium containing 10% FBS, and incubated with different concentrations of CSA (0, 1.0, and 10 μM , respectively). The wound was observed and recorded until the wound healed.

Statistical analyses

All data were presented as means \pm standard errors of the means (SEMs). Student's t tests were used to determine the differences in data between groups, and $P < 0.05$ was considered statistically different. The results of RT-qPCR, invasion assay, scratch wound healing assay and flow cytometry assay shown were representative of three independent experiments.

Results

Characterization of hESCs and hiPSCs

HiPSCs from villous cells were generated as previously reported [25]. Both hESCs and hiPSCs were maintained in the undifferentiated state (Fig. 1a). We performed immunostaining for the pluripotent marker OCT4 on hESCs and hiPSCs and as expected, we observed OCT4 positive staining of hESCs and hiPSCs (Fig. 1c, 1d). We also used flow cytometry to identify hESCs and hiPSCs that were positive for the trophoblast marker KRT7, and found that the expression of KRT7 was low, and that no HLA-G expression was detected in these cells (Fig. 1c, 1d).

Differentiation of hESCs and hiPSCs into EVT cells

Y27632 was important for cell attachment as a Rho-associated protein kinase (ROCK) inhibitor [16]. Matrigel was induced outgrowth of EVT cells from placental explants [26]. A recent research also found that decidua-derived NRG1 promoted EVT formation in placental explants [27]. In addition, the TGF- β inhibitor A83-01 promoted differentiation of CTB cells into EVT-like cells [16].

According to the method described previously [16], we cultured h hESCs and hiPSCs in a medium containing NRG1, A83-01, Y27632 and matrigel to induce differentiation based on the protocol shown in Fig. 2a. We found that the hESCs and hiPSCs changed from a colony-like morphology to an epithelial-like morphology at day 3 (Fig. 2b), and began to form cyst-like structures at day 6 (Fig. 2b).

Sorting and culturing of induced HLA-G-KRT7 double-positive hESC-EVT and hiPSC-EVT cells

We analyzed the double HLA-G + and KRT7 + cells by flow cytometry at day 9 of induction (Fig. 2c), and found that the induction efficiency of hESCs and hiPSCs differentiation into EVT cells was different, but no significant difference between these two cell types was observed (Fig. 2d) ($P \geq 0.05$). We also compared the induction efficiency of hESCs and hiPSCs cultured in different culture dishes, and found that the six-well cluster dishes was better than the 10 cm cell culture dish with regard to differentiation efficiency (Fig. S2a, 2b, 2c).

We first cultured the double HLA-G + and KRT7 + positive cells (i.e. hESC-EVT and hiPSC-EVT cells) obtained through flow cytometry in EVT basal medium, and found that the conditions did not sustain the survival of these derived cells, and most of them were not attached (data not shown). Therefore, we tested different culture conditions, and found that Y27632 and FBS were important for cell attachment and proliferation (Fig. 3a). Also, we realized that the derived cells needed to be seeded in a pre-coated with matrigel for 30 min. After hESC-EVT and hiPSC-EVT cells were passed 3–5 times, we found that these cells underwent epithelial-mesenchymal transition (Fig. S2d).

Characterization of HLA-G+/KRT7 + positive hESC-EVT and hiPSC-EVT cells

We next characterized the double HLA-G+/KRT7 + positive hESC-EVT and hiPSC-EVT cells with regard to gene expressions and biological functions. RT-qPCR analysis revealed that compared to the undifferentiated hESC and hiPSC cells, hESC-EVT and hiPSC-EVT cells has significantly lower expression of OCT4 (shown at day 0) but higher expression of HLA-G, ITGA5, and KRT7 (shown at day 9) (Fig. 3b). Consistent with the above observations, immunofluorescence staining revealed that these cells strongly expressed KRT7 (Fig. 3c), HLA-G (Fig. 3d) and ITGA5 (an EVT maker) (Fig. 3e). These results were in line with the observations from the primary cultured trophoblast cells (Fig. S1a) and the HTR-8/SVneo (an immortalized extravillous trophoblast cell line) (Fig. S1b). Additionally, the expression of matrix

metalloproteinases (MMPs), such as MMP 2 and MMP 9, which participate in human early trophoblast invasion through degrading the extracellular matrix (ECM), was significantly increased in the hESC-EVT and hiPSC-EVT cells compared to the hESC/hiPSC control ($P \leq 0.05$) (Fig. 3f). These findings argue that the induced double HLA-G+/CK7 + cells were EVT cells.

CsA promotes invasion of hESC-EVT and hiPSC-EVT cells

We next tested the effect of CsA on the invasion capability of hESC-EVT and hiPSC-EVT cells using the matrigel-based transwell assay. The induced hESC-EVT and hiPSC-EVT cells in the presence of different concentrations of CsA (0, 1.0, and 10 μ M, respectively) were cultured in the upper insert. After incubation for 48 h, the number of cells migrating to the lower surface were counted. CsA significantly increased the invasion capability of hESC-EVT (Fig. 4a, 4b) and hiPSC-EVT (Fig. 4c, 4d) cells in a dose dependent manner. Hence, CsA promotes the invasion of hESC-EVT and hiPSC-EVT cells.

CsA promotes migration of hESC-EVT and hiPSC-EVT cells

We also used the scratch wound healing assay to examine the effect of CsA on the migration capability of hESC-EVT and hiPSC-EVT cells. CsA significantly decreased the gap of the wound by migrating hESC-EVT (Fig. 5a, 5b) and hiPSC-EVT (Fig. 5c, 5d) cells in a dose-dependent manner. Further observations revealed that the gap of the wound was almost disappeared 12 h ~ 15 h after treatment with treatments of 1.0 μ M and 10 μ M of CsA, respectively, while in the vehicle control group, the gap of the wound was closed after 20h ~ 24 h. Hence, CsA promotes the migration of hESC-EVT and hiPSC-EVT cells.

Discussion

In this study, we derived EVT cells from hESCs and hiPSCs in vitro through incubation with a combination of various molecules, including Y-27632, A83-01, NRG1 and matrigel. The hESC-EVT and hiPSC-EVT cells we generated strongly expressed HLA-G and KRT7, markers of EVTs. Furthermore, we found that CsA promoted the invasion and migration of hESC-EVT and hiPSC-EVT cells, providing direct evidence for clinical application of CsA in treatment of pregnancy-related diseases such as PE, which are etiologically linked to deficient function of EVT cells.

In 2018, Okae et al derived human TS cells from blastocysts and the first-trimester placentas, and showed that TS cells could differentiate into EVT cells efficiently on a matrigel-supplemented medium in vitro [16]. Another study successfully used a micromesh culture technique to induce TS cells from trophoderm-like cysts [28], and confirmed that the TS cells differentiate into EVT cells using Okae's method. It is noteworthy that Turco et al adopted an in vitro culture system to establish the trophoblast organoids, and the trophoblast organoids generated an invasive and migratory HLA-G + EVT cells according to Okae's protocol [29]. Unlike the studies reported by Okae et al, we induced hiPSCs isolated from human villus and hESCs to differentiate into EVT cells rather than TS cells treated with the same chemicals used in their studies. We found that hiPSCs and hESCs gave rise to EVT-like cells as evidenced by high expression of HLA-G and ITGA5 in EVT-like cells and low expression of OCT4. Nonetheless, our flow cytometry

analysis suggested that the induction efficiency in our study was much lower than that reported in Okae' studies. One of the underlying reasons is that these studies used different cells for induction: human TS cells used in previous studies and hESCs/hiPSCs used in our study. However, since the double positive EVT cells generated in our study were much like the primary EVT cells obtained from the first-trimester placentas (Fig. S1a). In addition, the proportion of double positive EVT cells generated in our study was higher than that of the primary EVT cells obtained from the first-trimester placentas by flow cytometry (Fig. S1c). We believe that our system is suitable for the study of EVT cell functions in vitro. While the hESCs or hiPSCs treated with BMP4 differentiate into trophoblast-like cells, the BMP4-induced TB-like cells were mostly ST cells rather than EVT cells [25]. Since a possible trophoblast stem cell state may be presented during hESCs/hiPSCs differentiation into trophoblast cells, these TB-like cells could further differentiate into ST cells and EVT cells [30–31].

CsA is widely used for immunological rejection after organ transplantation. Recent studies have shown that CsA can be used to maintain the maternal-fetal tolerance and regulate trophoblast function. Our previous study showed that CsA improves the invasion adhesion and adhesion of mouse pre-implantation embryos by up-regulating MMP9 and integrin $\beta 3$ [32]. In line with the above observations, a study from another group revealed that a low concentration of CsA enhances growth and invasion of the human first-trimester trophoblast cells in vitro through activating MAPK/ERK1/2 signal pathway [20]. In addition, animal experiments showed that the low dose of CsA significantly reduces the mouse embryo absorption rate and improve pregnancy outcome in a spontaneous abortion (RSA) murine model [22], thus supporting those in vitro findings. As well known, the invasive EVT cells of the first trimester play an essential role in arterial remodeling process; insufficient invasion or migration of EVT cells contributes to PE development, fetal growth restriction (FGR), and RSA [6–7] [33]. However, the effects of CsA on EVT cell function is not clear during placenta development. In the present study, we treated the hiPSC-EVT and hESC-EVT cells with different concentrations of CsA, and found that CsA dose-dependently promoted the invasion and migration of hiPSC-EVT and hESC-EVT cells. Although the underlying mechanisms remains to be elucidated, our findings provide direct molecular basis of clinical application of CsA in the prevention and treatment of EVT cells dysfunction-related pregnancy complications.

To the best of our knowledge, this was a research that derived EVT cells from hESCs and hiPSCs without using BMP4. Since the ethical problems, primary trophoblast cells are difficult to obtain from human blastocysts and placental tissues. Furthermore, the isolate trophoblast cells cannot survive for a long time in vitro [12–13]. However, our study showed that the hESC-EVT and hiPSC-EVT cells could survive and proliferate under a culture condition containing 20% FBS and Y27632. When these cells were passed several times, their morphology underwent epithelial-mesenchymal transition (EMT) (Fig. S2d). These induced EVT cells gradually changed to obtain a fibroblast-like morphology. Previous studies found that the process of EMT was important for the migration and invasion of EVT cells in the human first-trimester, involved the attachment to the basement membrane and the degradation of the extracellular matrix [34–35]. Hence, the migration or invasion capacity of these derived EVT cells may highly linked with the process of EMT. Although the induction efficiency in this study was low, our study described an

in vitro cell system that can be used to study the maternal arterial remodeling process and disorders related to dysfunctional EVT cells.

Conclusion

In summary, we established EVT cells derived from hESCs and hiPSCs through induction by several factors without BMP4. These hESC-EVT and hiPSC-EVT cells represent a new cell model for investigating the function of EVT cells and mechanism of pregnancy-related disorders associated with EVT. Also, our findings that CsA promotes the invasion and migration of EVT cells provide molecular basis for clinical application of CsA in the prevention and treatment of EVT cells dysfunction-related pregnancy complications.

Abbreviations

TE: Trophoctoderm; TSc: Trophoblast stem cell; CTB: Cytotrophoblast; STB: Syncytiotrophoblast; EVT: Extravillous trophoblast; hiPSC: Human induced pluripotent stem cell; hESC: Human embryonic stem cell; PE: Pre-eclampsia; RAS: Recurrent spontaneous abortion; FGR: Fetal growth restriction; CsA: Cyclosporin A; MMP2: Matrix metalloproteinase-2; MMP9: Matrix metalloproteinase-9; NRG1: Human neuregulin-1; KSR: Knock out serum replacement; KRT7: Cytokeratin7; HLA-G: Human leukocyte antigen-G; ITGA5: Integrin alpha 5; GAPDH: Glyceraldehyde 3-phosphate dehydrogenase; EMT: Epithelial-mesenchymal transition

Declarations

Acknowledgments

We thank Prof. Jun Wang and Prof. Wangwei Cai for useful advice. We would like to thank Prof. Duanqing Pei and Dr. Lu Xiao for providing H1 cell line and HTR-8/SVneo cell line, as well as we also thank all donors for participating in this study.

Author Contributions

YHH and YLM designed the research and provided financial support. JXW and PL conducted the experiments. JXW, PL and SNT performed statistical analyses. WHZ, JLM, JL, BYW and DL contributed placental material. J.X.W wrote the manuscript. All authors read and approved the final manuscript.

Founding

This study was supported by the Major Science and Technology Program of Hainan Province (No. ZDKJ2017007), the National Natural Science Foundation of China (No.81460236) and the Hainan Provincial Natural Science Foundation of China (No. 2019CXTD408).

Availability of data and materials

All data generated or analyzed during this study are included in this article and supplementary information files.

Ethics approval and consent to participate

The study protocol was approved by the Ethics Committee of The First Affiliated Hospital of Hainan Medical University (2017-KY-001). The human placentas in this study were obtained from the department of Obstetrics and Gynecology, the First Affiliated Hospital of Hainan Medical University. All participants signed informed consent forms in this research.

Consent for publication

Not applicable.

Competing interests

The authors declare that they have no competing interests.

References

- [1]. Aplin John D. Developmental cell biology of human villous trophoblast: current research problems [J]. *Int. J. Dev. Biol.*, 2010, 54: 323-9.
- [2]. Pijnenborg R, Anthony J, Davey D A, et al. Placental bed spiral arteries in the hypertensive disorders of pregnancy [J]. *Br J Obstet Gynaecol*, 1991, 98: 648-55.
- [3]. Burton Graham J, Jauniaux Eric, Charnock-Jones D Stephen. The influence of the intrauterine environment on human placental development [J]. *Int J. Dev. Biol.*, 2010, 54: 303-12.
- [4]. Pijnenborg R, Vercruysse L, Hanssens M. The uterine spiral arteries in human pregnancy: facts and controversies [J]. *Placenta*, 2006, 27: 939-58.

- [5]. He Nannan, van Iperen Liesbeth, de Jong Danielle, et al. Human Extravillous Trophoblasts Penetrate Decidual Veins and Lymphatics before Remodeling Spiral Arteries during Early Pregnancy [J]. PLoS ONE, 2017, 12: e0169849.
- [6]. Windsperger Karin, Dekan Sabine, Pils Sophie, et al. Extravillous trophoblast invasion of venous as well as lymphatic vessels is altered in idiopathic, recurrent, spontaneous abortions [J]. Hum. Reprod, 2017, 32: 1208-1217.
- [7]. Burke Suzanne D, Karumanchi S Ananth. Spiral artery remodeling in preeclampsia revisited [J]. Hypertension, 2013, 62: 1013-4.
- [8]. Brosens Ivo, Puttemans Patrick, Benagiano Giuseppe. Placental bed research: I. The placental bed: from spiral arteries remodeling to the great obstetrical syndromes [J]. Am. J. Obstet. Gynecol, 2019, 221: 437-456.
- [9]. Steinberg Marissa L, Robins Jared C. Cellular Models of Trophoblast Differentiation [J]. Semin. Reprod. Med., 2016, 34: 50-6.
- [10]. Carter A M. Animal models of human placentation—a review [J]. Placenta, 2007, null: S41-7.
- [11]. Orendi K, Kivity V, Sammar M, et al. Placental and trophoblastic in vitro models to study preventive and therapeutic agents for preeclampsia [J]. Placenta, 2011, null: S49-54.
- [12]. Frank H G, Morrish D W, Pötgens A, et al. Cell culture models of human trophoblast: primary culture of trophoblast—a workshop report [J]. Placenta, 2001, null: S107-9.
- [13]. Stenqvist Ann-Christin, Chen Ting, Hedlund Malin, et al. An efficient optimized method for isolation of villous trophoblast cells from human early pregnancy placenta suitable for functional and molecular studies [J]. Am. J. Reprod. Immunol, 2008, 60: 33-42.
- [14]. Thomson J A, Itskovitz-Eldor J, Shapiro S S, et al. Embryonic stem cell lines derived from human blastocysts [J]. Science, 1998, 282: 1145-7.
- [15]. Schulz L C, Ezashi T, Das P, et al. Human embryonic stem cells as models for trophoblast differentiation [J]. Placenta, 2008, null: S10-6.
- [16]. Okae Hiroaki, Toh Hidehiro, Sato Tetsuya, et al. Derivation of Human Trophoblast Stem Cells [J]. Cell Stem Cell, 2018, 22: 50-63.e6.
- [17]. Turco Margherita Y, Gardner Lucy, Kay Richard G, et al. Trophoblast organoids as a model for maternal-fetal interactions during human placentation [J]. Nature, 2018, 564: 263-267.
- [18]. Piao Hai-Lan, Wang Song-Cun, Tao Yu, et al. Cyclosporine A enhances Th2 bias at the maternal-fetal interface in early human pregnancy with aid of the interaction between maternal and fetal cells [J]. PLoS

ONE, 2012, 7: e45275.

[19]. Wang Song-Cun, Yu Min, Li Yan-Hong, et al. Cyclosporin A promotes proliferating cell nuclear antigen expression and migration of human cytotrophoblast cells via the mitogen-activated protein kinase-3/1-mediated nuclear factor- κ B signaling pathways [J]. *Int J Clin Exp Pathol*, 2013, 6: 1999-2010.

[20]. Wang S-C, Tang Ch-L, Piao H-L, et al. Cyclosporine A promotes in vitro migration of human first-trimester trophoblasts via MAPK/ERK1/2-mediated NF- κ B and Ca²⁺/calcineurin/NFAT signaling [J]. *Placenta*, 2013, 34: 374-80.

[21]. Zhao Hong-Bo, Wang Can, Li Rui-Xia, et al. E-cadherin, as a negative regulator of invasive behavior of human trophoblast cells, is down-regulated by cyclosporin A via epidermal growth factor/extracellular signal-regulated protein kinase signaling pathway [J]. *Biol. Reprod.*, 2010, 83: 370-6.

[22]. Du Mei-Rong, Dong Lin, Zhou Wen-Hui, et al. Cyclosporin A improves pregnancy outcome by promoting functions of trophoblasts and inducing maternal tolerance to the allogeneic fetus in abortion-prone matings in the mouse [J]. *Biol. Reprod*, 2007, 76: 906-14.

[23]. James Joanna L, Stone Peter R, Chamley Lawrence W. The isolation and characterization of a population of extravillous trophoblast progenitors from first trimester human placenta [J]. *Hum. Reprod*, 2007, 22: 2111-9.

[24]. Clabault H el ene, Laurent Laetitia, Sanderson J Thomas, et al. Isolation and Purification of Villous Cytotrophoblast Cells from Term Human Placenta [J]. *Methods Mol. Biol*, 2018, 1710: 219-231.

[25]. Wei Yanxing, Zhou Xiaohua, Huang Wenhao, et al. Generation of trophoblast-like cells from the amnion in vitro: A novel cellular model for trophoblast development [J]. *Placenta*, 2017, 51: 28-37.

[26]. Miller R K, Genbacev O, Turner M A, et al. Human placental explants in culture: approaches and assessments [J]. *Placenta*, 2005, 26: 439-48.

[27]. Fock Valerie, Plessl Kerstin, Draxler Peter, et al. Neuregulin-1-mediated ErbB2-ErbB3 signalling protects human trophoblasts against apoptosis to preserve differentiation [J]. *J. Cell. Sci.*, 2015, 128: 4306-16.

[28]. Li Zhuosi, Kurosawa Osamu, Iwata Hiroo. Establishment of human trophoblast stem cells from human induced pluripotent stem cell-derived cystic cells under micromesh culture [J]. *Stem Cell Res Ther*, 2019, 10: 245.

[29]. Turco Margherita Y, Gardner Lucy, Kay Richard G, et al. Trophoblast organoids as a model for maternal-fetal interactions during human placentation [J]. *Nature*, 2018, 564: 263-267.

[30]. Li Yingchun, Moretto-Zita Matteo, Soncin Francesca, et al. BMP4-directed trophoblast differentiation of human embryonic stem cells is mediated through a Δ Np63⁺ cytotrophoblast stem cell state [J].

Development, 2013, 140: 3965-76.

[31]. Horii Mariko, Li Yingchun, Wakeland Anna K, et al. Human pluripotent stem cells as a model of trophoblast differentiation in both normal development and disease [J]. Proc. Natl. Acad. Sci. U.S.A., 2016, 113: E3882-91.

[32]. Huang Yuan-Hua, Ma Yan-Lin, Ma Lin, et al. Cyclosporine A improves adhesion and invasion of mouse preimplantation embryos via upregulating integrin $\beta 3$ and matrix metalloproteinase-9 [J]. Int J Clin Exp Pathol, 2014, 7: 1379-88.

[33]. Soares Michael J, Chakraborty Damayanti, Kubota Kaiyu, et al. Adaptive mechanisms controlling uterine spiral artery remodeling during the establishment of pregnancy [J]. Int. J. Dev. Biol., 2014, 58: 247-59.

[34]. E Davies Jessica, Pollheimer Jürgen, Yong Hannah E J, et al. Epithelial-mesenchymal transition during extravillous trophoblast differentiation [J]. Cell Adh Migr, 2016, 10: 310-21.

[35]. Godde Nathan J, Galea Ryan C, Elsum Imogen A, et al. Cell polarity in motion: redefining mammary tissue organization through EMT and cell polarity transitions [J]. J Mammary Gland Biol Neoplasia, 2010, 15: 149-68.

Figures

Figure 1. Characterization of hESCs and hiPSCs.

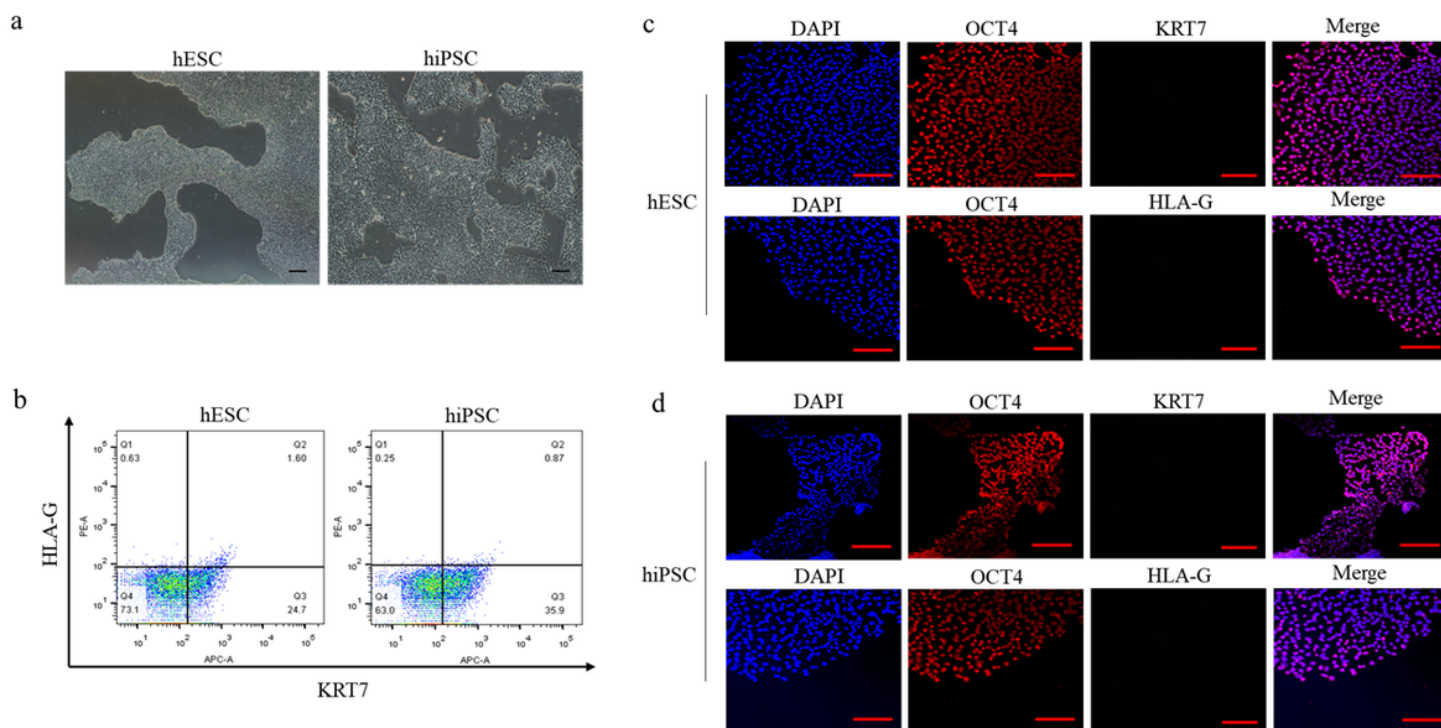


Figure 1

Characterization of hESCs and hiPSCs. (a) Morphology of isolated hESCs (H1) and hiPSCs. Scale bar, 200 μ m. (b) Flow cytometry analysis of hESCs and hiPSCs positive for KRT7+ and HLA-G+, respectively. (c&d) Immunostaining images showing hESCs and hiPSCs positive for the stem cell marker OCT4, trophoblast cell marker KRT7 and EVT cell marker HLA-G. Scale bar, 50 μ m.

Figure 2. Differentiation of hESCs and hiPSCs into EVT cells.

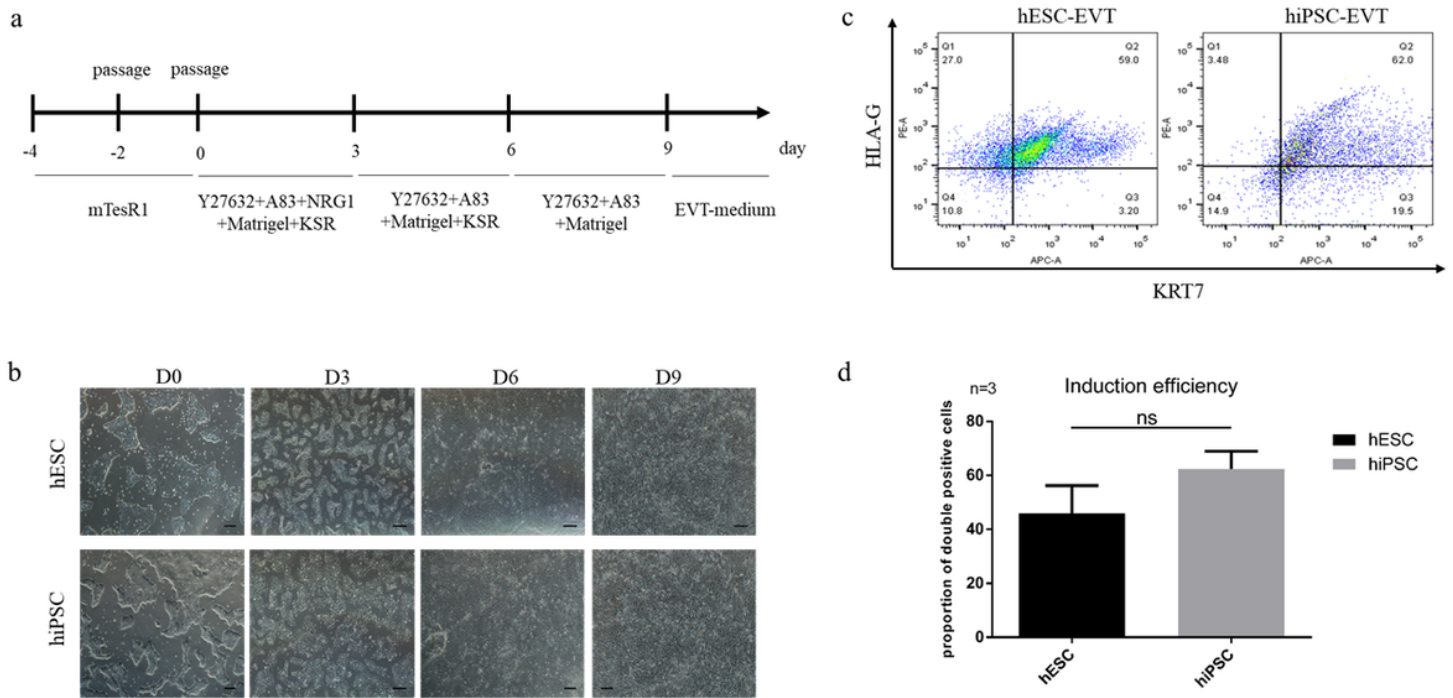


Figure 2

Differentiation of hESCs and hiPSCs into EVT cells. (a) Schematic representation of the protocol used for direct induction of differentiation of hESCs and hiPSCs into EVT cells. The EVT medium contains Y27632, A83-01, NRG1, matrigel and KSR at day 0. At day 3, this medium was replaced with another medium without NRG1. At day 6, the medium was replaced with another medium without NRG1 and KSR. The EVT-like cells were harvested at day 9. (b) Images showing morphological changes of hESCs and hiPSCs after differentiation induction at day 0, 3, 6 and 9, respectively. The cells have an epithelial-like morphology. Scale bar, 200 μ m. (c) Flow cytometry analysis of HLA-G+ and KRT7+ cells derived from the differentiation of hESCs and hiPSCs at day 9. (d) Percentage of KRT7 and HLA-G positive cells derived from hESCs and hiPSCs. * $P < 0.05$ compared with the control. Data shown were compiled from three independent experiments.

Figure 3. Characterization of double HLA-G+/KRT7+ EVT cells derived from differentiation of hESCs and hiPSCs.

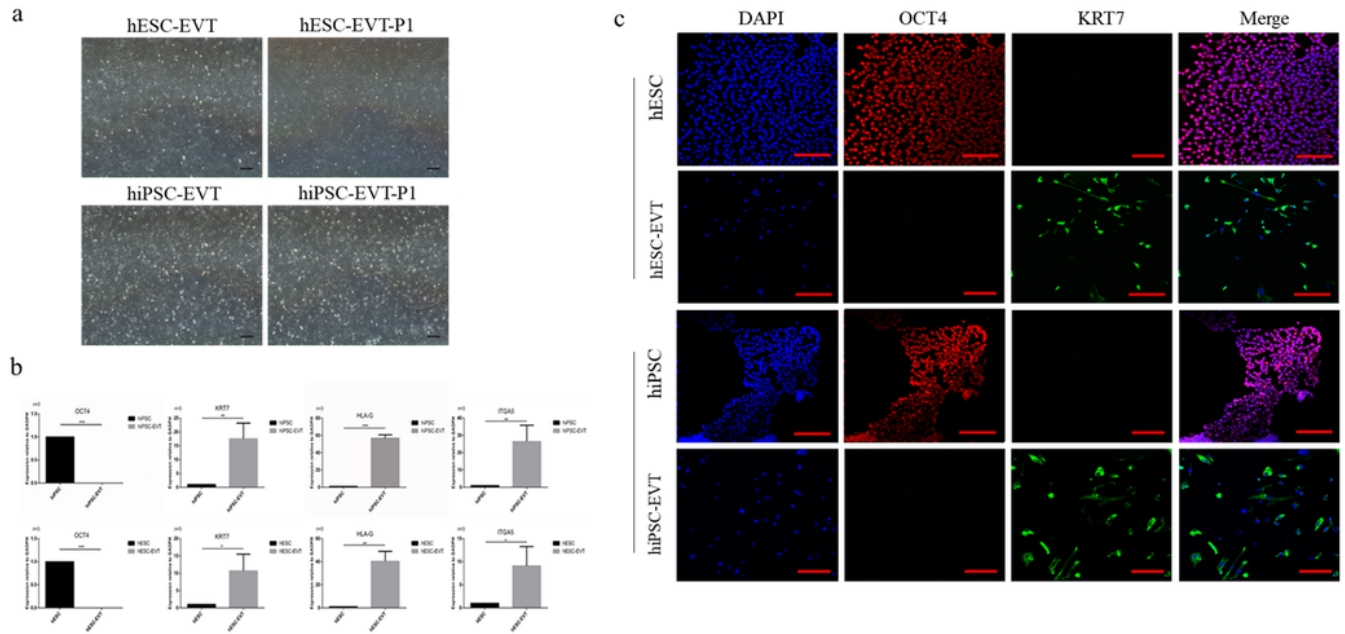


Figure 3. Characterization of double HLA-G+/KRT7+ EVT cells derived from differentiation of hESCs and hiPSCs.

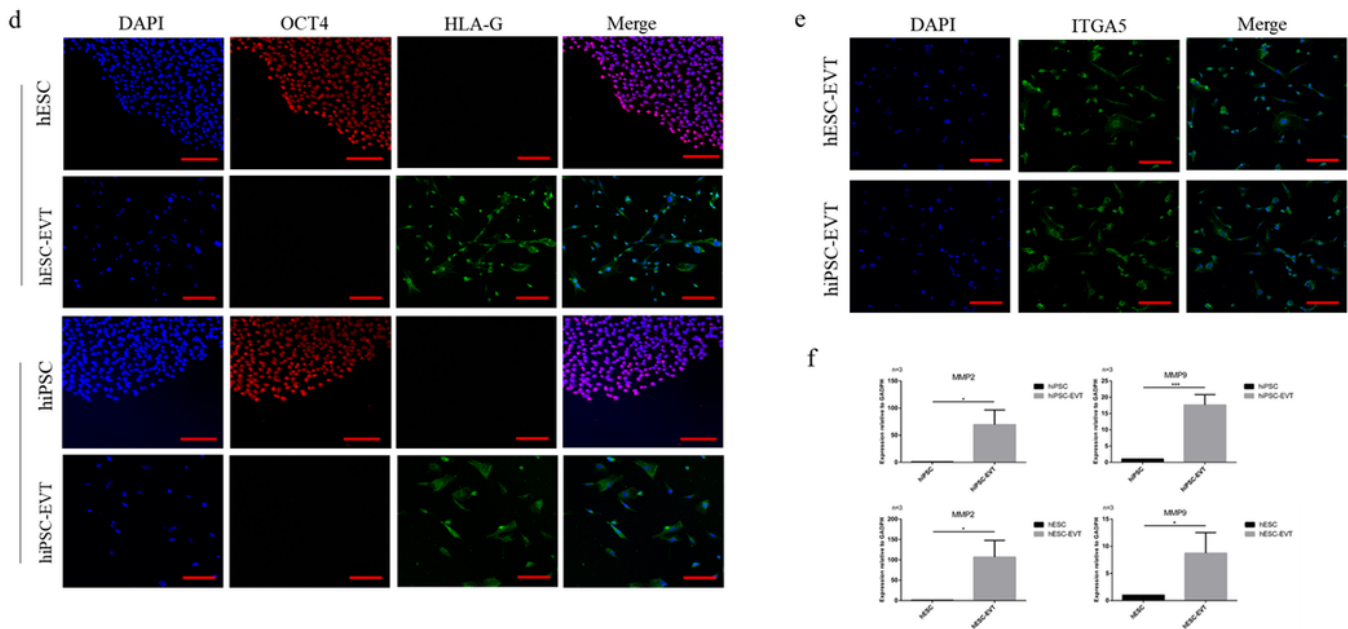


Figure 3

Characterization of double HLA-G+/KRT7+ EVT cells derived from differentiation of hESCs and hiPSCs. (a) Phase contrast images showing double HLA-G+/KRT7+ hiESC-EVT and hiPSC-EVT cells. Please note that EVT cells maintained epithelial-like morphology. Scale bar, 200 μ m. (b) RT-qPCR analysis of expression levels of pluripotency gene OCT4, trophoblast specific gene KRT7, and EVT specific genes HLA-G and ITGA5 in hESCs and hiPSCs (day 0) and double HLA-G+/KRT7+ hESC-EVT/hiPSC-EVT cells

(day 9). Values were normalized to GADPH and the gene expression at day 0 serves as a control. * $P < 0.05$ compared with the control. Data shown were compiled from three independent experiments. (c&d) Immunostaining for OCT4, KRT7, ITGA5 and HLA-G in HLA-G+/KRT7+ EVT cells. Nuclei were stained with DAPI. Scale bar, 50 μm . (f) RT-qPCR analysis of expression levels of MMP2 and MMP9 in hESCs and hiPSCs (day 0) and double HLA-G+/KRT7+ hESC-EVT/hiPSC-EVT cells (day 9). Values were normalized to GADPH and the gene expression at day 0 serves as a control. * $P < 0.05$, ** $P < 0.01$ and *** $P < 0.001$ compared with the control. Data shown were compiled from three independent experiments.

Figure 4. CsA promotes invasion of hESC-EVT and hiPSC-EVT cells.

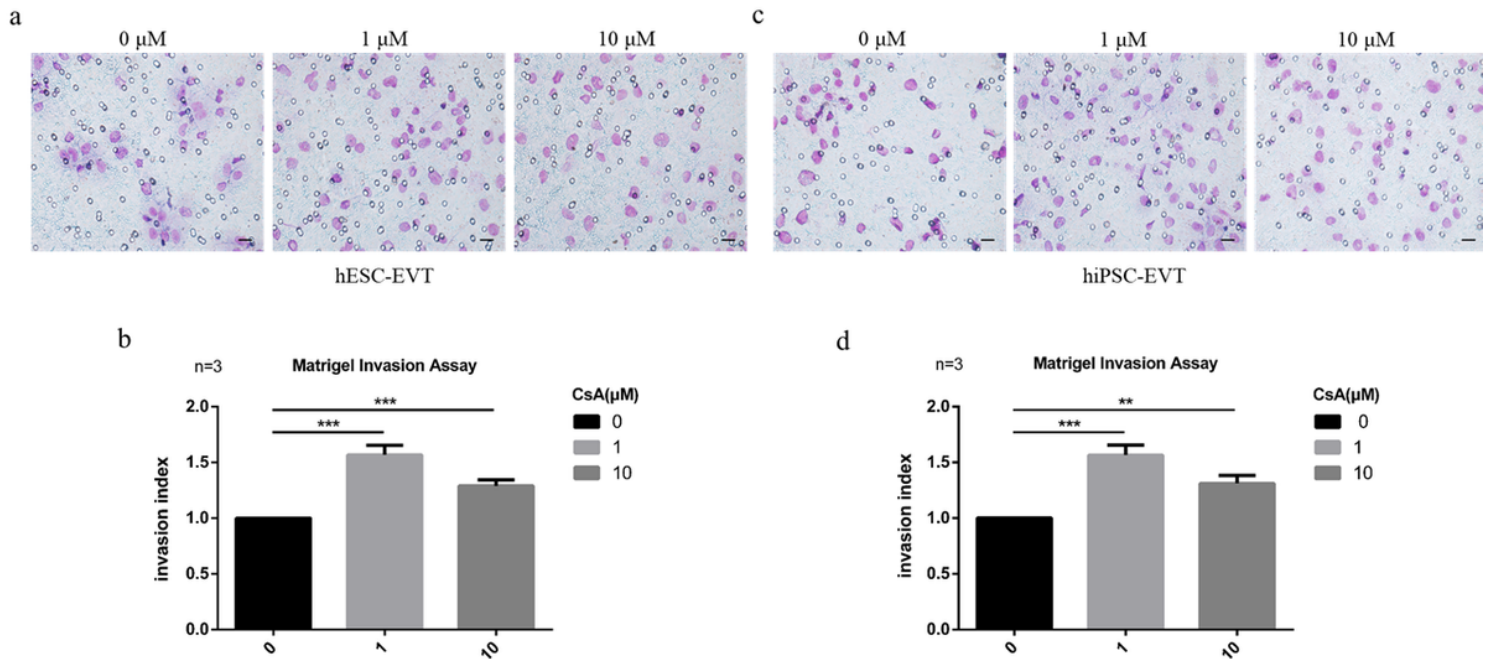


Figure 4

CsA promotes invasion of hESC-EVT and hiPSC-EVT cells. (a&c) hESC-EVT cells (a) and hESC-EVT cells (c) were cultured on transwell inserts for 48 h in the medium containing different concentrations of CsA as indicated. Representative images showing the invasion of EVT cells through the matrigel-coated membranes. Magnification, 400x. Scale bar, 20 μm . (b&d) The invasion index of hESC-EVT cells (b) and hiPSC-EVT cells (d) under different conditions were normalized to the control. * $P < 0.05$, ** $P < 0.01$ and *** $P < 0.001$ compared to the vehicle controls. Data shown were compiled from three independent experiments, and are expressed as mean \pm SEM.

Figure 5. CsA promotes migration of hESC-EVT and hiPSC-EVT cells.

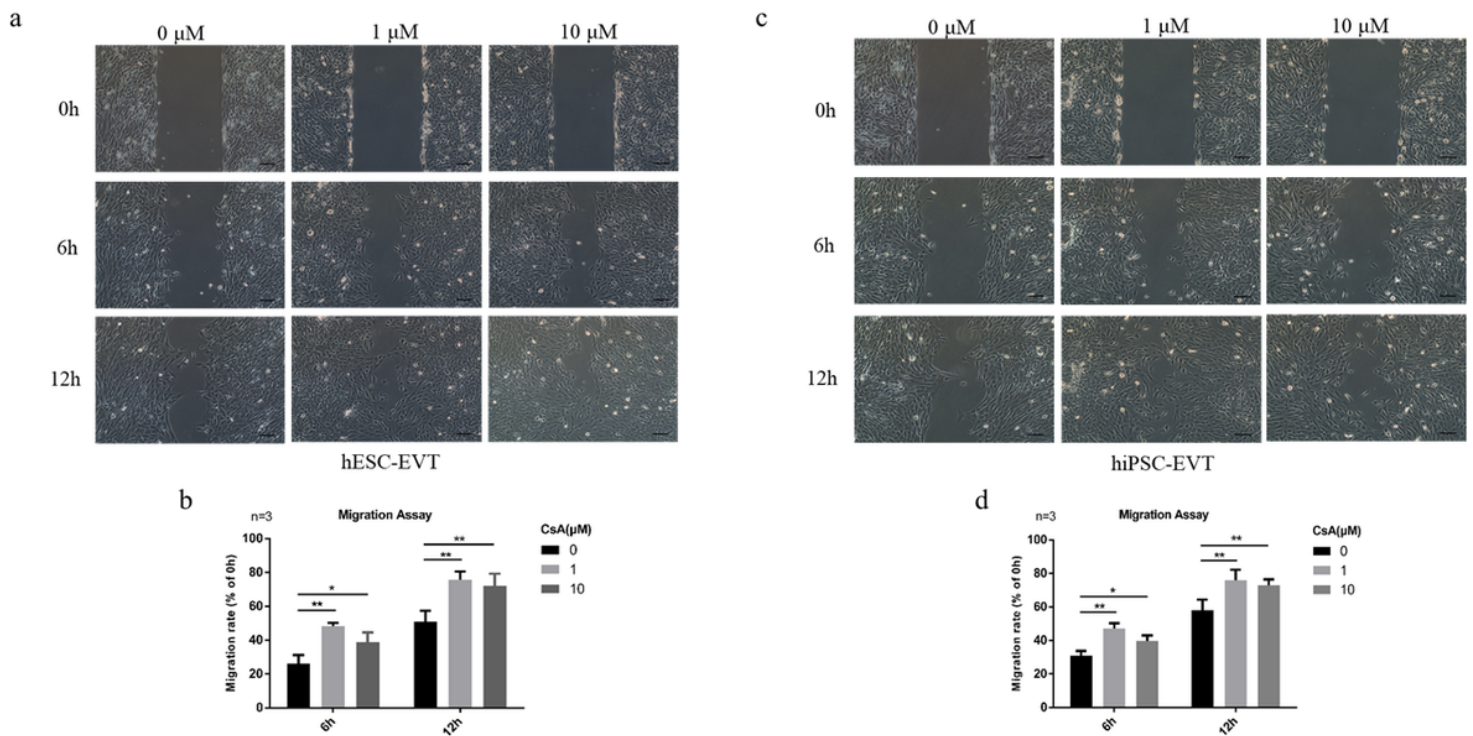


Figure 5

CsA promotes migration of hESC-EVT and hiPSC-EVT cells. (a&c) Analysis of the cell migration by the scratch wound healing assay. An open wound was generated by scratching cells at 90% confluency with a culture-insert. Treatments with different concentrations of CsA as indicated facilitated the migration. The distance between the wounds in the hESC-EVT and hiPSC-EVT cells was measured. Representative images were obtained at 0, 6, and 12 h after CsA treatments. (b&d) The migration rates of hESC-EVT and hiPSC-EVT cells under different treatment conditions were calculated using the following formula: (area of the wound at 0h – area of the wound at 6h or 12h)/area of the wound at 0h. * $P < 0.05$, ** $P < 0.01$ and *** $P < 0.001$, compared with the vehicle control. Data shown were compiled from three independent experiments, and are expressed as mean \pm SEM.

Supplementary Files

This is a list of supplementary files associated with this preprint. Click to download.

- [SupplementaryTableS3primers.docx](#)
- [SupplementaryFigures.pptx](#)
- [SupplementaryTableS2Antibodies.docx](#)
- [SupplementaryTableS1Reagentsorkits.docx](#)